



HAL
open science

Application of Fe-MFI zeolite catalyst in heterogeneous electro-Fenton process for water pollutants abatement

Thi Xuan Huong Le, Martin Drobek, Mikhael Bechelany, Julius Motuzas,
Anne Julbe, Marc Cretin

► To cite this version:

Thi Xuan Huong Le, Martin Drobek, Mikhael Bechelany, Julius Motuzas, Anne Julbe, et al.. Application of Fe-MFI zeolite catalyst in heterogeneous electro-Fenton process for water pollutants abatement. *Microporous and Mesoporous Materials*, 2019, 278, pp.64-69. 10.1016/j.micromeso.2018.11.021 . hal-02146496

HAL Id: hal-02146496

<https://hal.umontpellier.fr/hal-02146496>

Submitted on 23 Nov 2020

HAL is a multi-disciplinary open access archive for the deposit and dissemination of scientific research documents, whether they are published or not. The documents may come from teaching and research institutions in France or abroad, or from public or private research centers.

L'archive ouverte pluridisciplinaire **HAL**, est destinée au dépôt et à la diffusion de documents scientifiques de niveau recherche, publiés ou non, émanant des établissements d'enseignement et de recherche français ou étrangers, des laboratoires publics ou privés.

26 pollutants, avoiding the use of any non-recyclable soluble Fe^{2+} salt classically required as EF
27 catalyst.

28

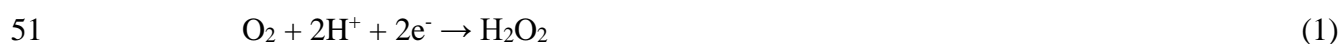
29 **KEYWORDS.** *Heterogeneous electro-Fenton process, Fe-MFI zeolite, Mineralization, Dye*
30 *removal, Water treatment.*

31

32 **1. Introduction**

33 Water pollution leads to many serious problems that affect the entire biosphere on the
34 planet Earth [1] [2]. Hence, the wastewater treatment for the reuse of polluted water sources
35 remains one of the great concerns of current scientific research. Many different methods have
36 been applied either at lab-scale or industrial scale for the abatement of water pollutants by *e.g.*
37 adsorption [3], bacterial degradation [4], radiolytic degradation [5], filtration [6], electrodialysis
38 technology [7] [8], *etc.* However, these methods still present several limitations related namely
39 to the formation of secondary wastes, or production of highly toxic intermediates such as 2-
40 naphthol or 1-amino-2-naphthol, because of low treatment efficiency [5]. To overcome these
41 bottlenecks, Advanced Oxidation Processes (AOPs) have been developed, including diverse
42 technologies combining *e.g.* UV-light with strong oxidizing agents like O_3 or H_2O_2 in photolysis
43 [9], photo-Fenton by ferrioxalate-Fenton/UV-A and TiO_2 /UV-A processes [10] [11] or other
44 Fenton-based processes [12]. Among these methods, electro-Fenton (EF) process is known as an
45 optimal approach to decompose completely the persistent organic pollutants (POPs) in aqueous
46 media. This method involves the production of hydroxyl radicals ($\cdot\text{OH}$), as powerful oxidizing
47 agents, which can destroy and transform POPs into low toxicity compounds such as short chain
48 carboxylic acids (formic or acetic acids) with their further mineralization into CO_2 and H_2O [13]
49 [14]. The process involves two steps [15]:

50 i) Production of hydrogen peroxide from oxygen reduction:



52 ii) and EF process:



55 In homogeneous EF process, a soluble iron catalyst is added to the solution and
56 regenerated through the reduction of Fe^{3+} (Eq. 3). However, adding Fe^{2+} to treated waters leads
57 to another pollution risk for the environment because ferrous ions remain in the solution and
58 their removal is not a trivial task. Consequently, in recent years the heterogeneous EF process
59 has attracted a special attention as it avoids the usage of homogeneous catalyst. Hassan &
60 Hameed proved that using Fe–ball clay (Fe–BC) as heterogeneous EF catalyst led to 99%
61 decolorization of anthraquinone dye Reactive Blue 4 with initial concentration of 50 mg L^{-1} after
62 140 min treatment [16]. This catalyst was prepared from $\text{FeSO}_4 \cdot 7\text{H}_2\text{O}$ via impregnation method
63 combined with calcination step at 500°C . In addition, pyrite has been applied commonly due to
64 its low cost and abundance. Numerous pollutants were degraded by usage of pyrite in EF
65 process, for example antibiotic levofloxacin [17], azo dye – the (4-amino-3-hydroxy-2-p-
66 tolylazo-naphthalene-1-sulfonic acid) [18], or tyrosol [19]. In addition, other catalyst sources like
67 iron alginate gel beads [20], Fe_2O_3 modified kaolin [21], $\gamma\text{-FeOOH}$ [22], pyrrhotite [23] have
68 been also successfully applied in EF process. Recently our research group has studied
69 heterogeneous EF catalyst based on hierarchical CoFe-Layered Double Hydroxide (CoFe-LDH)
70 synthesized by *in-situ* solvothermal method. It exhibited an outstanding stability with high TOC
71 removal even after multiple reaction cycles [24].

72 In order to find other possible alternatives in the area of heterogeneous EF process, in this
73 work we propose for the first time the application of EF system based on carbon felt (CF)
74 substrates modified with iron-rich MFI zeolite nanoseeds prepared by solvothermal microwave-
75 assisted synthesis method. This approach is of a particular interest because it combines the
76 attractive properties of both CF and zeolite material. CF has been known as an effective material
77 for EF process because of its low cost, good conductivity, high mechanical stability, porosity and

78 surface area which supply plentiful active redox sites [25] [26]. Concerning the zeolites, in the
79 area of wastewater treatment, they are typically used as adsorbers taking advantage of their high
80 specific surface areas. In addition large variety of functionalities, such as acid-base or redox
81 centres can be incorporated into the zeolite structures to confer them catalytic properties enabling
82 a chemical abatement of waste water. In this respect, zeolites with incorporated heteroatoms, *i.e.*
83 Fe, could be used as heterogeneous catalyst in EF treatment of water pollutants, avoiding the use
84 of any non-recyclable soluble Fe^{2+} salt classically used in EF process and at the same time
85 enabling a repetitive utilisation of the system in consecutive reaction cycles.

86 The efficiency and stability of the cathode was investigated by the treatment of a dye
87 solution contaminated by Acid Orange 7 (AO7) which was chosen as a model azo dye molecule.
88 This work contributes to the development of processes for the treatment of effluents containing
89 biorefractory pollutants in general with a particular attention devoted to heterogeneous EF
90 process using iron-rich zeolite materials.

91

92 **2. Experimental**

93 **2.1. Reagents and materials**

94 Tetraethyl orthosilicate (TEOS, 98%), tetrapropyl ammonium hydroxide (TPAOH, 20
95 wt% aqueous solution), AO7 (Aid Orange 7 also called Orange II sodium salt), anhydrous
96 sodium sulphate (Na_2SO_4 , 99.0 – 100.5%), graphite powder and iron (II) sulphate hepta-hydrate
97 ($\text{FeSO}_4 \cdot 7\text{H}_2\text{O}$, 99%) were purchased from Sigma-Aldrich. Iron (III) acetylacetonate ($\text{Fe}(\text{acac})_3$,
98 99.9%) was obtained from Alfa Aesar and sodium hydrogen carbonate (NaHCO_3 , $\geq 99.5\%$) from
99 ACS, Karlsruhe. The carbon felt was bought from A Johnson Matthey Co., Germany. All these
100 reagents were used as received, without further purification.

101 **2.2. Preparation of MFI zeolite based catalyst**

102 The MFI zeolite based catalyst was produced according to a protocol described elsewhere
103 (Motuzas et al. 2017). The molar concentration of the mother solution was set at $(x/2) \text{Fe}_2\text{O}_3$:

104 100 SiO₂: 40 TPAOH: 1950 H₂O: 400 C₂H₅OH, where x was adapted to the required molar
105 amount of Fe in the MFI zeolite structure. The selected Fe-rich MFI zeolite has been synthesized
106 from solutions having Si/Fe atomic ratio equal to 50 (2 at% Fe). It must be noted the synthesis of
107 MFI zeolites from solutions with Si/Fe atomic ratios < 50 failed due to undesirable gelation of
108 the reaction sols. For the sake of comparison, a pure silicalite-1 zeolite material (0 at.% Fe) has
109 been prepared from an iron-free solution. After aging the sols for 24 h at 25 °C (under
110 continuous stirring), they were poured in autoclaves and heated in a commercial laboratory
111 microwave oven (Milestone ETHOS 1600). The hydrothermal treatment was conducted in two
112 steps. First, the closed autoclaves were irradiated for 90 min at 80 °C with a microwave power of
113 250 W. Then the power was increased up to 400 W for heating the autoclaves up to 180 °C for
114 60 min. Finally, the autoclaves were cooled down to 50 °C before opening. The formed solid
115 products were separated by centrifugation at 9500 rpm (JOUAN B4i) and washed twice with
116 distilled water and centrifuged again. The as-washed MFI zeolite powders were dispersed in
117 water (3.7 wt.%) and the resulting suspensions were used to impregnate the commercial carbon
118 felts (CF). The prepared MFI@CF composite materials were dried for 4 h at 155 °C and then
119 submitted to a calcination treatment. The calcination has been carried out under flowing nitrogen
120 (200 mL.min⁻¹) in a tubular furnace (Vecstar Ltd) at 550 °C for 4 h, with heating and cooling
121 rates of 5 °C min⁻¹. Non calcined MFI@CF composite materials were also used immediately
122 after drying at 155 °C.

123 **2.3. Material characterizations**

124 Chemical and structural characterizations of the prepared materials have been performed
125 by scanning electron microscopy (SEM, Hitachi S-4800), X-ray diffraction (XRD) (PANalytical
126 Xpert-PRO diffractometer equipped with a X'celerator detector using Ni-filtered Cu-radiation)
127 and EDX analysis (Silicon Drift Detector (SDD), X-MaxN, Oxford Instrument) coupled to a
128 Zeiss EVO HD15 SEM analyzer. The N₂ sorption-desorption isotherms were measured with a
129 Micromeritics ASAP 2010 equipment (outgassing conditions: 200°C-12h).

130 **2.4. Heterogeneous electro-Fenton set-up**

131 The heterogeneous EF experiments were carried out in an open electrolytic cell with 250
132 mL capacity and a working volume of 200 mL. The cathode was either a commercial CF, noted
133 as raw CF, or a composite MFI@CF material with dimensions 1 cm * 2 cm * 1.27 cm. The
134 MFI@CF was prepared according to the method described in section 2.2. The anode was a Pt
135 foil setting parallel with the cathode at a distance of 3 cm. AO7 was used as a model pollutant
136 and its concentration was fixed at 0.1 mM for all experiments in this study. Na₂SO₄ (50 mM)
137 was added into dye solution which plays the role of supporting electrolyte. The initial solution
138 pH was ~ 6.4 without any adjustment with H₂SO₄ or NaOH. Homogenization of the electrolysis
139 solution was ensured by a magnetic stirrer at 500 rpm. Compressed air was bubbled continuously
140 into the solution, starting 10 min before the beginning of electrolysis. Solution samples were
141 taken at regular treatment times (2 h, 4 h, 6 h and 8 h, respectively) to quantify the evolution of
142 the mineralization degree during EF treatment, via TOC analysis on a Shimadzu TOC-L analyzer
143 with 8-port sampler, supplied by pure oxygen at a flow rate of 200 mL min⁻¹. Calibration of the
144 analyzer was done by automatic dilution of standard TOC solutions (potassium
145 hydrogenophthalate) and inorganic carbon (sodium hydrogen carbonate). The decomposition of
146 AO7 was monitored by measuring the dye absorbance at $\lambda = 485$ nm, specific wavelength for
147 azo bond, using Spectrophotometer Jenway 6300 (Barioworld Scientific Ltd, Dunmow UK). The
148 absorbance of this bond was proportional to the AO7 concentration, according to the Beer-
149 Lambert law (calibration graph).

150 The catalyst stability was investigated by running experiments for 5 consecutive cycles.
151 Between each cycle, the MFI@CF was well washed by distilled water (15 $\mu\Omega$) and dried at 80
152 °C in an oven. The efficiency of treatment was evaluated by measuring the efficiency of the
153 washed electrode for a new TOC removal experiment.

154 **3. Results and discussion**

155 The strategy selected for the preparation of carbon felt electrodes modified by MFI
156 zeolite seeds (MFI@CF) involves two steps: (i) the growth of MFI zeolite nano-seeds by MW-
157 assisted heating and (ii) the deposition of these zeolite seeds, dispersed in aqueous suspension,
158 on commercial carbon felts. The as-prepared electrode material was used in heterogeneous
159 electro-Fenton (EF) process for the abatement of a model dye pollutant, acid Orange 7 (AO7).
160 The key aspects related to the efficiency of such a reaction system have been discussed hereafter
161 together with the characteristics of the electrodes. A special focus was devoted to evidence the
162 promising performance of iron-rich Fe-MFI@CF material, at near neutral pH, for a “green” EF
163 treatment of water pollutants, while avoiding the use of any non-recyclable soluble Fe^{2+} salt
164 classically required as EF catalyst.

165

166 **3.1. Preparation of MFI zeolite nanoseeds**

167 The MFI nano-seeds were prepared by a MW-assisted hydrothermal treatment, as
168 reported elsewhere (Motuzas et al. 2017). This procedure enables, within less than 3 h, the
169 production of MFI zeolite seeds with uniform size distribution. The SEM images in Fig. 1a
170 demonstrate that MFI zeolite morphology is influenced by the Fe concentration. The Fe-free (0
171 at.% Fe) MFI zeolite seeds (S-1) feature typical MFI type crystal morphology, while the Fe-rich
172 (FeS-1) MFI zeolite (2.33 at.% Fe in the solid, as determined by EDX analysis) exhibit
173 aggregated microstructure forming particles without sharp edges. It must be noted that when
174 comparing with their non-calcined analogues, calcination carried out under the nitrogen
175 atmosphere, does not lead to any detectable change of zeolite seeds morphology, neither for S-1
176 nor for FeS-1 (results not shown here).

177 A characteristic monoclinic MFI crystal structure has been confirmed by wide angle
178 XRD analysis for both S-1 and FeS-1 zeolite powders (Fig.1b). The slightly higher resolution of
179 the S-1 pattern translates its higher crystallinity degree in comparison with FeS-1 in which Fe
180 insertion slightly disturbs the construction of the MFI crystalline network. In addition it must be

181 noted that XRD analysis also confirmed the absence of detectable quantity of secondary phases
182 (i.e. extra-framework particles) like iron oxides, thus suggesting that the Fe species detected by
183 EDX analysis are mainly incorporated in the MFI particles as intra-framework species.

184

185 **3.2. Preparation of MFI@CF electrodes**

186 As described in the experimental section, the commercial carbon felts have been modified
187 by deposition of zeolite nanoseeds, thus forming composite MFI@CF material. SEM images of
188 both pristine and modified carbon felt are displayed in Fig.2. As in the case of pure zeolite seeds,
189 no difference was observed when comparing the morphology of MFI@CF non-calcined and after
190 treatment at 550°C under the nitrogen atmosphere. SEM observations confirmed a good
191 distribution of the zeolite nanoseeds covering nearly uniformly the surface of commercial carbon
192 felts. Previous studies on graphite felt modified by zeolite material proved that catalyst loading
193 affects noticeably the performance of the fabricated electrode. Once the mass of NaX zeolite on
194 the electrode increased from 0.03 g to 0.13 g, the electrochemical activity of the electrode
195 increased by 1.5 times [27]. In the present study, the catalyst loading was strictly controlled by
196 weighting electrode before and after modification during the preparation procedure. An
197 optimized electrode was obtained when its mass was kept nearly constant at 55+6 wt.% zeolite
198 loading after thorough washing to ensure that electrode was fully covered with Fe-MFI. Over
199 this amount no more zeolite material could be deposited on the carbon felt electrode. The
200 modification of pristine carbon felts ($S_{\text{BET}} \sim 0.1 \text{ m}^2 \text{ g}^{-1}$) with MFI zeolites led to an increase of
201 the specific surface area by more than 600 times, thanks to the high specific surface area of
202 zeolite nanoseeds, even before any calcination treatment (Table 1).

203 When the MFI@CF samples were subjected to a calcination treatment (550°C in N₂), an
204 additional increase of their active surface area was measured (Table 1), due to the decomposition
205 of the organic structure directing agent (SDA, TPAOH) in the zeolite channels. The required
206 neutral N₂ atmosphere for the calcination treatment (preserving the integrity of the CF) is less

207 efficient than a conventional oxidation in air for a complete evacuation of the SDA
208 decomposition species from the zeolite pores but should result at least in a detectable liberation
209 of zeolite channels. As expected, the SDA degradation resulted in an increase of the zeolite pore
210 volume (i.e. from $0.049 \text{ cm}^3 \text{ g}^{-1}$ to $0.057 \text{ cm}^3 \text{ g}^{-1}$ for non-calcined and calcined samples,
211 respectively). Hence, the modification of a raw CF with zeolite seeds, followed by its calcination
212 in N_2 atmosphere raised nearly 1000 times the specific surface area of the raw carbon cathode.
213 This finding has been further confirmed by TGA experiments (Fig. 3) carried out on the zeolite
214 seeds exhibiting $\sim 12\text{wt.}\%$ loss corresponding to the removal of the organic SDA from the
215 zeolite material. The slight weight difference $\sim 0.55\text{wt.}\%$ between the samples treated in air and
216 nitrogen was attributed to the presence of residual carbonaceous species on/in the zeolitic
217 material calcined in N_2 atmosphere (lower weight loss).

218

219 **3.3. Removal of AO7 by heterogeneous EF process using MFI@CF electrode**

220 The target of present study is performing the heterogeneous EF process to treat bio-
221 refractory pollutants in neutral medium (pH ~ 6.4). The effect of pH on AO7 degradation has
222 been carefully investigated in our previous studies about heterogeneous electro-Fenton (EF)
223 process using Fe-based LDH catalysts [24],[28]. It was shown that working at low pH values
224 (i.e. 2-3) led to the Fe leaching from heterogeneous catalysts, thus inducing significant
225 drawbacks for real environmental applications during wastewater treatment in industry. In
226 addition to undesirable iron precipitation, an alteration of industrial equipment in acidic medium
227 is predictable as well as a required basic treatment before discharging the solutions in the
228 environment. Similarly, working at high pH (over 7) reduces AO7 degradation efficiency
229 because of catalyst precipitation. Therefore, in this work, the neutral pH value of initial AO7
230 solution was kept unchanged in all experiments. In comparison with a raw CF electrode, the
231 higher surface area of MFI@CF electrode is expected to induce a higher quantity of H_2O_2
232 electrogenerated from dissolved oxygen according to Eq.1. Hence, more H_2O_2 should react with

233 the heterogeneous iron catalyst *via* EF process (Eq. 2) on Fe-MFI@CF electrode for the
234 production of oxidizing hydroxyl radicals attacking the AO7 molecules and leading to their
235 degradation. The decay kinetics of AO7 was monitored by measuring the dye absorbance at the
236 selected single wavelength $\lambda = 485$ nm, specific for azo bond. The blank tests in the absence of
237 Fe species were carried out at the same experimental condition as with the iron-based zeolite
238 catalyst. The complete degradation of 200 mL AO7 (0.1 mM) was achieved after 40 min contact
239 on the Fe-MFI@CF instead of more than 120 min on the non-modified raw CF one (Fig. 4a).
240 The AO7 removal on raw CF was explained by the anodic oxidation that occurred at the Pt anode,
241 through Eq. 4 from water oxidation [29]:



243 In order to evaluate the influence of anodic oxidation on the degradation of AO7,
244 experiments were performed using Pt as both cathode and anode. As observed in Fig. 4a, the
245 anodic oxidation led to the color removal of AO7 after 2 h. A similar result was obtained when
246 using a raw CF cathode and a Pt anode. Additional experiments carried out with S-1@CF
247 cathode led also to AO7 removal due to the synergetic effect of both anodic oxidation on the
248 electrode and strong adsorption efficiency of Fe-free MFI zeolite. Nearly 46 % of AO7 was
249 removed after 9 min by using Fe-free MFI zeolite cathode, which was 1.5 times higher than with
250 the bare cathode (~30 %). The fastest AO7 removal, *i.e.* EF process leading to the most efficient
251 dye elimination in aqueous medium, was observed when applying a Fe-MFI@CF cathode, thus
252 proving the efficiency of the carbon felt cathode modification for heterogeneous EF process. The
253 presence of iron in the zeolite framework accelerated the treatment efficiency; hence there was
254 69 % of the initial AO7 amount which was degraded in the same amount of time. This increase
255 resulted from the heterogeneous EF process enabling to generate more hydroxyl radicals ($\cdot\text{OH}$)
256 which are powerful oxidizing agents able to destroy and transform quickly AO7 dye molecules
257 [13], [14]. The interest of Fe-MFI modification is then to combine adsorption properties of the
258 porous material with electrocatalytic properties of iron for heterogeneous electro-Fenton as

259 already proposed in our previous work devoted to nitrogen-doped graphitized carbon electrodes
260 for biorefractory pollutant removal by homogeneous electro-Fenton (Le et al., 2017b). The AO7
261 degradation by hydroxyl radicals formed during the heterogeneous EF process followed a
262 pseudo-first order kinetic. The apparent rate constant was determined by plotting the
263 $\ln([AO7^0]/[AO7])$ vs. time [26]. A value of 0.226 min^{-1} was obtained for the Fe-MFI@CF
264 cathode; this value was nearly three times higher than those obtained for a MFI@CF electrode
265 (without any Fe catalytic sites), i.e. 0.0838 min^{-1} . In the experiment with raw CF, the anodic
266 oxidation contributed mainly for AO7 removal with a similar rate constant value of 0.078 min^{-1} .
267 This result strongly proved the important role of heterogeneous Fe-MFI catalyst for AO7
268 degradation. Moreover, this conclusion was once again confirmed via measuring TOC removal
269 (Fig. 4b). In fact, the TOC abatement reached 26.6 % after 8 hours reaction time with the Fe-
270 MFI@CF cathode calcined in nitrogen, while the abatement value do not overpass ~5% for the
271 raw CF cathode

272 As expected without any calcination step, the heterogeneous EF process yielded a
273 negative TOC removal. It was explained by the leaching of the organic SDA (TPAOH) from the
274 zeolite network after synthesis. The TOC removal went down to nearly – 20 % after 4 h and then
275 gradually climbed up due to the decomposition of organics by heterogeneous radicals. As
276 observed in Fig. 4c, the Fe-MFI@CF cathode calcined in nitrogen lost partially its catalytic
277 activity after 5 consecutive cycles. It was blamed for the gradual loss of Fe-MFI catalyst out
278 from the carbon electrode during EF experiments.

279 According to Figures 4a&b, AO7 degradation is achieved when using a relevant zeolite modified
280 carbon felt (Fe-MFI@CF treated at 550°C under N_2 atmosphere), in hetero-EF at circumneutral
281 pH, by a surface catalyzed process. In comparison with conventional EF systems, the large
282 increase of performance was ascribed to (i) surface-catalysed reaction which expands the
283 working pH window and avoids the precipitation of iron sludge appearing at neutral pH in
284 homogenous electro-Fenton technology, (ii) improvement of H_2O_2 production due to the increase

285 of the electroactive cathode surface area (accessible pore volume) which allows coupling both
286 adsorption and EF process (reactive electrochemically materials) and (iii) further improvement
287 of the adsorption capacity after calcination of the organic template in N₂. It is also important to
288 note that the Fe-MFI@CF cathode exhibited relatively good reusability after 5 degradation
289 cycles, indicating that the prepared material is a promising cathode for the removal of organic
290 pollutants by hetero-EF technology.

291 **4. Conclusion**

292 In this study, we have successfully prepared a novel zeolite modified electrode which is
293 active for heterogeneous electro-Fenton (EF) process. Iron-rich MFI zeolite nanoseeds have been
294 deposited at the surface of a commercial carbon felt (CF) thus forming a MFI@CF composite
295 material exhibiting an attractive activity as electrode (cathode) for direct *in-situ* formation of
296 H₂O₂ electrogenerated from dissolved oxygen. This highly reactive electrochemical material
297 allows a coupling of both adsorption and EF process. Indeed the presence of Fe-MFI seeds with
298 a size of 200 nm deposited on the electrodes played an essential role in the production of
299 hydroxyl radicals as highly reactive species for the removal of organics from the aqueous media.
300 The TOC removal reached 27 % after 8 hours at pH 6.5 in comparison with 5 % at raw electrode.
301 The iron rich Fe-MFI@CF cathode exhibited relatively good stability after several consecutive
302 cycles with a decrease of the catalytic activity of ~25% due to partial wash-out of the zeolite
303 seeds. Improvement of seed anchoring on electrode surface is currently under investigation in
304 our group, but this preliminary work is of huge interest as it clearly demonstrates the possibility
305 to develop heterogeneous electro-Fenton process at neutral pH instead of acidic pH in traditional
306 electro-Fenton systems. The present study contributes importantly to (i) develop novel
307 heterogeneous catalysts for the electro-Fenton process towards industrial applications in waste
308 water treatment; (ii) enrich the application field using designed porous materials.

309

310 **5. Acknowledgments.**

311 We gratefully acknowledge financial support from the ANR project
312 ECOTS/CELECTRON for the funding of this research.

313

314

315 **REFERENCES**

- 316 [1] P. R. Hunter, D. Zmirou-Navier, and P. Hartemann, “Estimating the impact on health of
317 poor reliability of drinking water interventions in developing countries,” *Sci. Total*
318 *Environ.*, vol. 407, no. 8, pp. 2621–2624, 2009.
- 319 [2] J. O. Back *et al.*, “Risk assessment to groundwater of pit latrine rural sanitation policy in
320 developing country settings,” *Sci. Total Environ.*, vol. 613–614, pp. 592–610, 2018.
- 321 [3] Q. Liu *et al.*, “Enhanced dispersion stability and heavy metal ion adsorption capability of
322 oxidized starch nanoparticles,” *Food Chem.*, vol. 242, no. August 2017, pp. 256–263,
323 2018.
- 324 [4] R. G. Saratale, G. D. Saratale, J. S. Chang, and S. P. Govindwar, “Bacterial decolorization
325 and degradation of azo dyes: A review,” *J. Taiwan Inst. Chem. Eng.*, vol. 42, no. 1, pp.
326 138–157, 2011.
- 327 [5] S. J. Zhang, H. Q. Yu, and Q. R. Li, “Radiolytic degradation of Acid Orange 7: A
328 mechanistic study,” *Chemosphere*, vol. 61, no. 7, pp. 1003–1011, 2005.
- 329 [6] Y. Chen and X. Song, “A phosphorylethanolamine-functionalized super-hydrophilic 3D
330 graphene-based foam filter for water purification,” *J. Hazard. Mater.*, vol. 343, pp. 298–
331 303, 2018.
- 332 [7] S. Melnikov, N. Sheldeshov, V. Zabolotsky, S. Loza, and A. Achoh, “Pilot scale complex
333 electro dialysis technology for processing a solution of lithium chloride containing organic
334 solvents,” *Sep. Purif. Technol.*, vol. 189, no. August, pp. 74–81, 2017.
- 335 [8] L. Han, Y. Liu, and J. W. Chew, “Boron transfer during desalination by electro dialysis,”
336 *J. Memb. Sci.*, vol. 547, no. August 2017, pp. 64–72, 2018.
- 337 [9] P. V. L. Reddy and K. H. Kim, “A review of photochemical approaches for the treatment
338 of a wide range of pesticides,” *J. Hazard. Mater.*, vol. 285, pp. 325–335, 2015.
- 339 [10] I. Arslan, I. A. Balcioglu, and D. W. Bahnemann, “Advanced chemical oxidation of
340 reactive dyes in simulated dyehouse effluents by ferrioxalate-Fenton/UV-A and TiO₂/UV-

- 341 A processes,” *Dye. Pigment.*, vol. 47, no. 3, pp. 207–218, 2000.
- 342 [11] Z. Frontistis *et al.*, “Photocatalytic (UV-A/TiO₂) degradation of 17 β -ethynylestradiol in
343 environmental matrices: Experimental studies and artificial neural network modeling,” *J.*
344 *Photochem. Photobiol. A Chem.*, vol. 240, pp. 33–41, 2012.
- 345 [12] E. Brillas, I. Sirés, and M. A. Oturan, “Electro-fenton process and related electrochemical
346 technologies based on fenton’s reaction chemistry,” *Chem. Rev.*, vol. 109, no. 12, pp.
347 6570–6631, 2009.
- 348 [13] T. X. H. Le *et al.*, “Toxicity removal assessments related to degradation pathways of azo
349 dyes: Toward an optimization of Electro-Fenton treatment,” *Chemosphere*, vol. 161, pp.
350 308–318, 2016.
- 351 [14] T. X. H. Le *et al.*, “Correlation between degradation pathway and toxicity of
352 acetaminophen and its by-products by using the electro-Fenton process in aqueous
353 media,” *Chemosphere*, vol. 172, pp. 1–9, 2017.
- 354 [15] T. X. H. Le *et al.*, “Nitrogen-Doped Graphitized Carbon Electrodes for Biorefractory
355 Pollutant Removal,” *J. Phys. Chem. C*, vol. 121, no. 28, pp. 15188–15197, 2017.
- 356 [16] H. Hassan and B. H. Hameed, “Fe-clay as effective heterogeneous Fenton catalyst for the
357 decolorization of Reactive Blue 4,” *Chem. Eng. J.*, vol. 171, no. 3, pp. 912–918, 2011.
- 358 [17] N. Barhoumi *et al.*, “Electrochemical mineralization of the antibiotic levofloxacin by
359 electro-Fenton-pyrite process,” *Chemosphere*, vol. 141, pp. 250–257, 2015.
- 360 [18] L. Labiadh, M. A. Oturan, M. Panizza, N. Ben Hamadi, and S. Ammar, “Complete
361 removal of AHPS synthetic dye from water using new electro-fenton oxidation catalyzed
362 by natural pyrite as heterogeneous catalyst,” *J. Hazard. Mater.*, vol. 297, pp. 34–41, 2015.
- 363 [19] S. Ammar *et al.*, “Degradation of tyrosol by a novel electro-Fenton process using pyrite as
364 heterogeneous source of iron catalyst,” *Water Res.*, vol. 74, pp. 77–87, 2015.
- 365 [20] O. Iglesias, J. Gómez, M. Pazos, and M. Á. Sanromán, “Electro-Fenton oxidation of
366 imidacloprid by Fe alginate gel beads,” *Appl. Catal. B Environ.*, vol. 144, pp. 416–424,

- 367 2014.
- 368 [21] A. Özcan, A. Atılır Özcan, Y. Demirci, and E. Şener, “Preparation of Fe₂O₃modified
369 kaolin and application in heterogeneous electro-catalytic oxidation of enoxacin,” *Appl.*
370 *Catal. B Environ.*, vol. 200, pp. 361–371, 2017.
- 371 [22] X. Q. Wang, C. P. Liu, Y. Yuan, and F. B. Li, “Arsenite oxidation and removal driven by
372 a bio-electro-Fenton process under neutral pH conditions,” *J. Hazard. Mater.*, vol. 275,
373 pp. 200–209, 2014.
- 374 [23] Y. Li *et al.*, “Microbial fuel cells using natural pyrrhotite as the cathodic heterogeneous
375 Fenton catalyst towards the degradation of biorefractory organics in landfill leachate,”
376 *Electrochem. commun.*, vol. 12, no. 7, pp. 944–947, 2010.
- 377 [24] S. O. Ganiyu *et al.*, “A hierarchical CoFe-layered double hydroxide modified carbon-felt
378 cathode for heterogeneous electro-Fenton process,” *J. Mater. Chem. A*, vol. 5, no. 7, pp.
379 3655–3666, 2017.
- 380 [25] T. X. Huong Le, M. Bechelany, and M. Cretin, “Carbon felt based-electrodes for energy
381 and environmental applications: A review,” *Carbon N. Y.*, vol. 122, pp. 564–591, 2017.
- 382 [26] T. X. H. Le, M. Bechelany, J. Champavert, and M. Cretin, “A highly active based
383 graphene cathode for the electro-fenton reaction,” *RSC Adv.*, vol. 5, no. 53, pp. 42536–
384 42539, 2015.
- 385 [27] X. Wu *et al.*, “Effect of NaX zeolite-modified graphite felts on hexavalent chromium
386 removal in biocathode microbial fuel cells,” *J. Hazard. Mater.*, vol. 308, pp. 303–311,
387 2016.
- 388 [28] S. O. Ganiyu *et al.*, “Electrochemical mineralization of sulfamethoxazole over wide pH
389 range using FeII/FeIII/LDH modified carbon felt cathode: Degradation pathway, toxicity
390 and reusability of the modified cathode,” *Chem. Eng. J.*, vol. 350, pp. 844–855, 2018.
- 391 [29] S. Hammami, N. Bellakhal, N. Oturan, M. a. Oturan, and M. Dachraoui, “Degradation of
392 Acid Orange 7 by electrochemically generated •OH radicals in acidic aqueous medium

393 using a boron-doped diamond or platinum anode: A mechanistic study,” *Chemosphere*,
394 vol. 73, no. 5, pp. 678–684, 2008.

395

396